

Landslides (2014) 11:859–875
 DOI 10.1007/s10346-013-0416-2
 Received: 10 July 2012
 Accepted: 16 May 2013
 Published online: 14 June 2013
 © Springer-Verlag Berlin Heidelberg 2013

Benni Thiebes · Rainer Bell · Thomas Glade · Stefan Jäger · Julia Mayer · Malcolm Anderson · Liz Holcombe

Integration of a limit-equilibrium model into a landslide early warning system

Abstract Landslides are a significant hazard in many parts of the world and exhibit a high, and often underestimated, damage potential. Deploying landslide early warning systems is one risk management strategy that, amongst others, can be used to protect local communities. In geotechnical applications, slope stability models play an important role in predicting slope behaviour as a result of external influences; however, they are only rarely incorporated into landslide early warning systems. In this study, the physically based slope stability model CHASM (Combined Hydrology and Stability Model) was initially applied to a reactivated landslide in the Swabian Alb to assess stability conditions and was subsequently integrated into a prototype of a semi-automated landslide early warning system. The results of the CHASM application demonstrate that for several potential shear surfaces the Factor of Safety is relatively low, and subsequent rainfall events could cause instability. To integrate and automate CHASM within an early warning system, international geospatial standards were employed to ensure the interoperability of system components and the transferability of the implemented system as a whole. The CHASM algorithm is automatically run as a web processing service, utilising fixed, predetermined input data, and variable input data including hydrological monitoring data and quantitative rainfall forecasts. Once pre-defined modelling or monitoring thresholds are exceeded, a web notification service distributes SMS and email messages to relevant experts, who then determine whether to issue an early warning to local and regional stakeholders, as well as providing appropriate action advice. This study successfully demonstrated the potential of this new approach to landslide early warning. To move from demonstration to active issuance of early warnings demands the future acquisition of high-quality data on mechanical properties and distributed pore water pressure regimes.

Keywords Landslide · Early warnings system · CHASM (Combined Hydrology and Stability Model) · Physically based · Modelling · Web processing service · Web notification service · Swabian Alb

Introduction

Landslides are a world-wide problem, often with an underestimated damage potential. The significance of landslide hazards is demonstrated by the high levels of annual damage that some countries experience. Turner (1996) states that the economic damage in the USA amounts to US\$ 1–2 billion, in addition to 25–50 fatalities. In China, Yin (2009) estimates direct annual economic losses amount to approximately 10 billion RMB (approximately US\$ 1.3 billion) with some 900 fatalities. Even in Germany with its relatively low fraction of high mountain areas, the annual damage has been calculated to be US\$ 150 million (Krauter 1992) 20 years ago. In an attempt to reduce these losses, landslide susceptibility, hazard and risk maps are prepared to provide spatial information and to aid spatial planning (e.g. Chung 2008; Goetz et al. 2011; Guzzetti et al. 2005; Rossi et al. 2010).

Where hazardous areas cannot be avoided, engineering slope stabilisation can be applied to secure potential landslide bodies, and protect the local population and their socio-economic activities. In this geo-engineering context, quantitative landslide simulations have a long tradition, and such models are frequently applied for back analysis and the planning of protective structures (Barla et al. 2004; Janbu 1996). However, slope stabilisation is in many cases not feasible either because of cost and/or scale—the affected areas are too large. Under these circumstances, landslide monitoring and early warning can at least temporarily replace structural slope stabilisation measures, while providing an appropriate level of protection (Palm et al. 2003). Early warning systems can form an essential part of landslide damage prevention and risk management by alerting the local population to evacuate endangered areas when slope failures are imminent (Dikau and Weichselgartner 2005). Examples of local-scale landslide early warning system have been described by many authors (e.g. Badoux et al. 2009; Blikra 2008; Clark et al. 1996; Froese et al. 2005; Willenberg et al. 2002). Essentially, these systems are based on monitoring systems for slope movement or landslide triggering factors, such as rainfall and/or pore water pressures. Alarm thresholds are either defined by expert judgement and interpretation of monitoring data (Blikra 2008; Froese et al. 2005; Krauter et al. 2007; Lauterbach et al. 2002; Macfarlane et al. 1996; Ruch 2009; Yin et al. 2010) or calculated by quantitative predictive models (Capparelli and Tiranti 2010; Iovine et al. 2010; Sirangelo and Braca 2004). Thus, a direct integration of monitoring data into numerical models to simulate early warnings, as expected by Stähli and Bartelt (2007) for the next generation of warning systems, has not been reported thus far.

In this paper, the application of a physically based landslide model CHASM (Combined Hydrology and Stability Model) to a reactivated landslide in the Swabian Alb is presented. The model is used to assess likely shear surfaces of landslide reactivations and the influence of rainfall and groundwater on slope stability. Subsequently, CHASM is implemented as an automated early warning model based on real-time hydrological monitoring data and historic quantitative rainfall forecasts. The CHASM model is integrated into a prototypic semi-automated early warning system which, from a technical standpoint, is capable of providing early warning to relevant experts and decision-makers. The objective of the paper is thus to outline, and demonstrate, the structure of a landslide early warning system and the associated potential of the approach. Future use of the methodology to for the issuance of ‘live’ early warnings would require the acquisition of high-quality data on mechanical properties and distributed pore water pressure regimes.

Whilst the research described here is part of a PhD research (Thiebes 2011, 2012), this paper focuses on a more detailed exposition, and demonstration, of the landslide early warning system that was developed.

Study area

Swabian Alb

The study area is located in the Swabian Alb, a mountain range in southwest Germany (Fig. 1). The lithology of the Swabian Alb primarily comprises Jurassic clay underlying marl and limestone strata, the latter forming a steep escarpment which stretches in a southwest to northeast direction for some 200 km. Elevations reach 1,000 m in the western part, and between 600 and 800 m in the central and eastern sections. Landslides are a common geomorphological feature in the region due to lithological conditions (Terhorst 1997) and to triggers of rainfall events, snow melting and earthquakes (Meyenfeld 2009). In total, approximately 30,000 landslide bodies of various sizes and ages are assumed to be present in the entire Swabian Alb (Bell 2007). The most recent large landslide event was the 'Mössinger Bergrutsch' that took place in 1983. During this event, approximately 6 million cubic meters of material were triggered by exceptionally wet conditions (Bibus 1986; Funderinger 1985; Schädel and Stober 1988). Additional landslides in this area were reported in May and June 2013 after

exceptionally long lasting rainfall. As a consequence, 24 houses were evacuated. Several authors emphasise the importance of landslides for the relocation of the cuesta escarpment and the evolution to the present landscape (Bibus 1999; Bleich 1960; Terhorst 1997), but they also represent a significant current geo-hazard (Bell et al. 2006; Kallinich 1999; Kreja and Terhorst 2005; Neuhäuser and Terhorst 2007; Papathoma-Köhle et al. 2007; Terhorst and Kreja 2009).

Lichtenstein-Unterhausen

This paper focuses on a reactivated landslide in Lichtenstein-Unterhausen, south of the city of Reutlingen. The slope under investigation faces south-west and occupies an area of approximately 0.5 km² (Fig. 1). The highest altitude is approximately 780 m a.m.s.l., the river in the valley is at an elevation of approximately 465 m a.m.s.l. The local study area comprises two large landslide bodies with head scarps at approximately 660 m a.m.s.l. Today, steep slopes and higher elevations areas are dominantly occupied by forest, while lower slopes feature pasture. Settlement activity on the slope under investigation started in the 1960s and

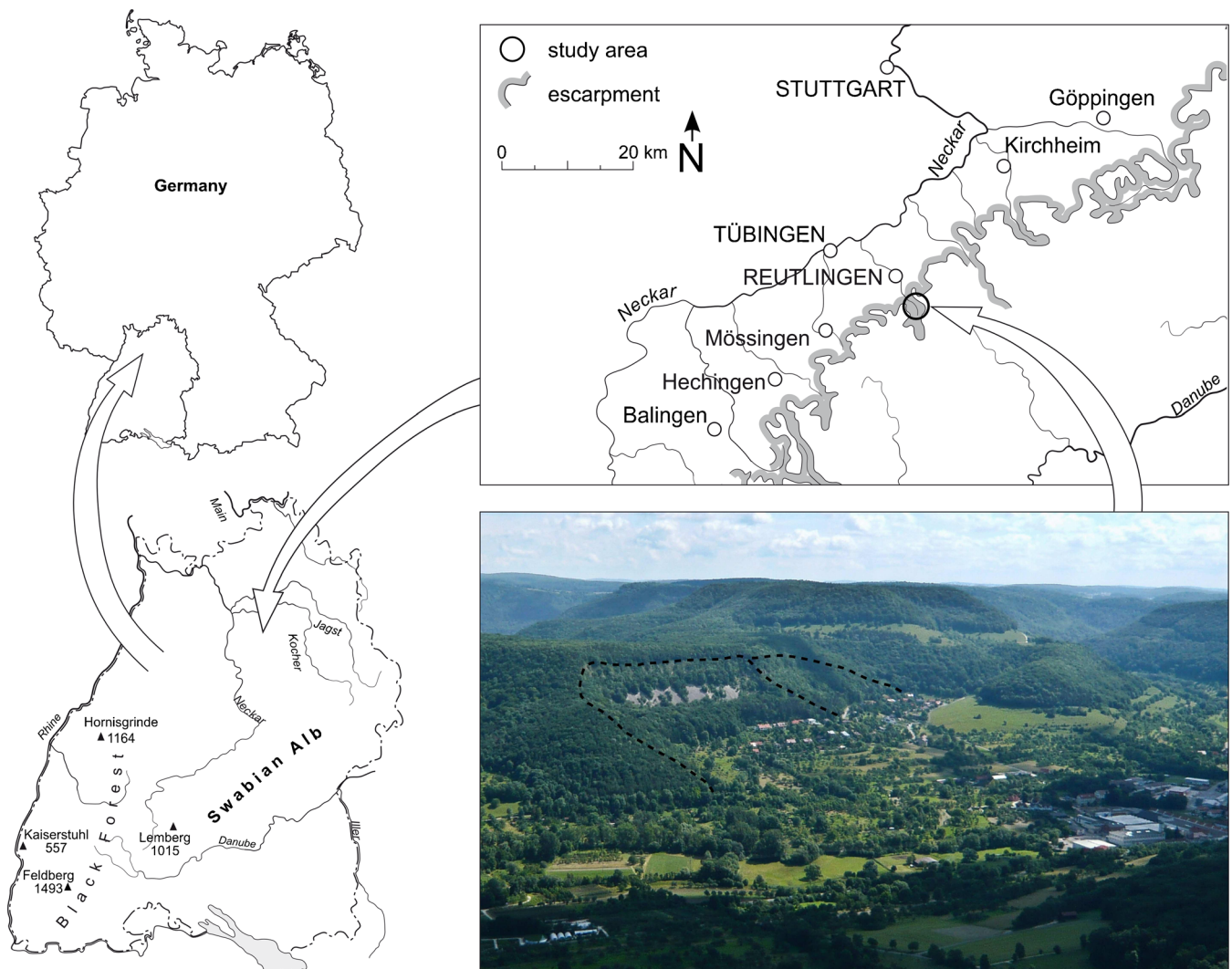


Fig. 1 The study area Lichtenstein-Unterhausen in the Swabian Alb with an oblique view on the landslide under investigations (*dashed lines* show assumed landslide boundaries)

continues today. The local development plan obligates all construction works to be preceded by a technical geological survey (Schönwälder 2005 in Bell 2007); however, at least one building suffers frequent cracking due to slope movements.

Geology

The lithology of the study area primarily consists of Upper and Middle Jurassic sediments dipping south west by 1–2° (Leser 1982) (Fig. 2). Slopes are mostly covered by slope debris from Pleistocene solifluction and activity of shallow landslides. Fluvial deposits and tufa of Late Glacial and Holocene age cover the valley bottom. At the highest elevations in the study area, massive limestones are intersected by thin marl interstices (Untere Massenkalk Formation—joMu) of the Upper Jurassic. Below approximately 730 m a.m.s.l., a marl stratum (Zementmergel—ki5) with an average thickness of 20 m overlies the dominantly marl stratum of Lacunosamergel (ki1) located above approximately 670 m a.m.s.l. An Upper Jurassic stratified limestone (Wohlgeschichtete Kalk Formation—ox2) forms a plateau with an elevation of approximately 660 m a.m.s.l. This stratum comprises a series of stratified limestone beds intersected by thin layers of lime marl beds. The underlying marl stratum (Impressamergel—ox1) forms steep slopes and can be found up to approximately 610 m a.m.s.l. However, the material is often locally relocated further downslope due to rotational landslide processes. The ox1 stratum is characterised by an alternation of marl and marl lime beds. Upper sections mainly consist of massive limestone beds, while lower

sections also comprise clay marls. Below the ox1 stratum, the Medium Jurassic Ornatenton (cl) is present which consists of dark claystones with 5–15 % of calcium carbonate. The material is often deeply weathered and prone to landslide processes (Ohmert et al. 1988). A thin stratum of Bathonian clays (bt), sometimes termed Dentalienton, can be assumed for the study area (Ohmert et al. 1988); however, no outcrops are present. Bajocian strata bj3, bj2 and bj1 were mapped in the north-western part of the study area, and comprise clays marlstones and sandy limestones with clay sections. At several locations, volcanic tuff is displayed in the map, originating from tertiary volcanic activity.

Geomorphology

A comprehensive geomorphological map based on field mapping and the analysis of a 1 m DTM was established by Bell (2007) (Fig. 3). The slope is dominated by two large landslide bodies of which the western is significantly larger (approximately 2.5 million m³ and 950,000 m³, respectively). Landslide deposits of the larger mass reach the valley floor and altered the course of the river Echaz. Both landslide bodies feature a step-like morphology with flat areas in the head area below the main scarp. Two younger landslides with approximate volumes of 700,000 m³ and 6500 m³, respectively, are located on the western landslide body. These movements comprise reactivation of material affected by the older phase of landslide activity. A recent landslide event with an approximate volume of 700 m³ took place in 1984, when a small rotational landslide was triggered by construction works not adapted to local conditions.

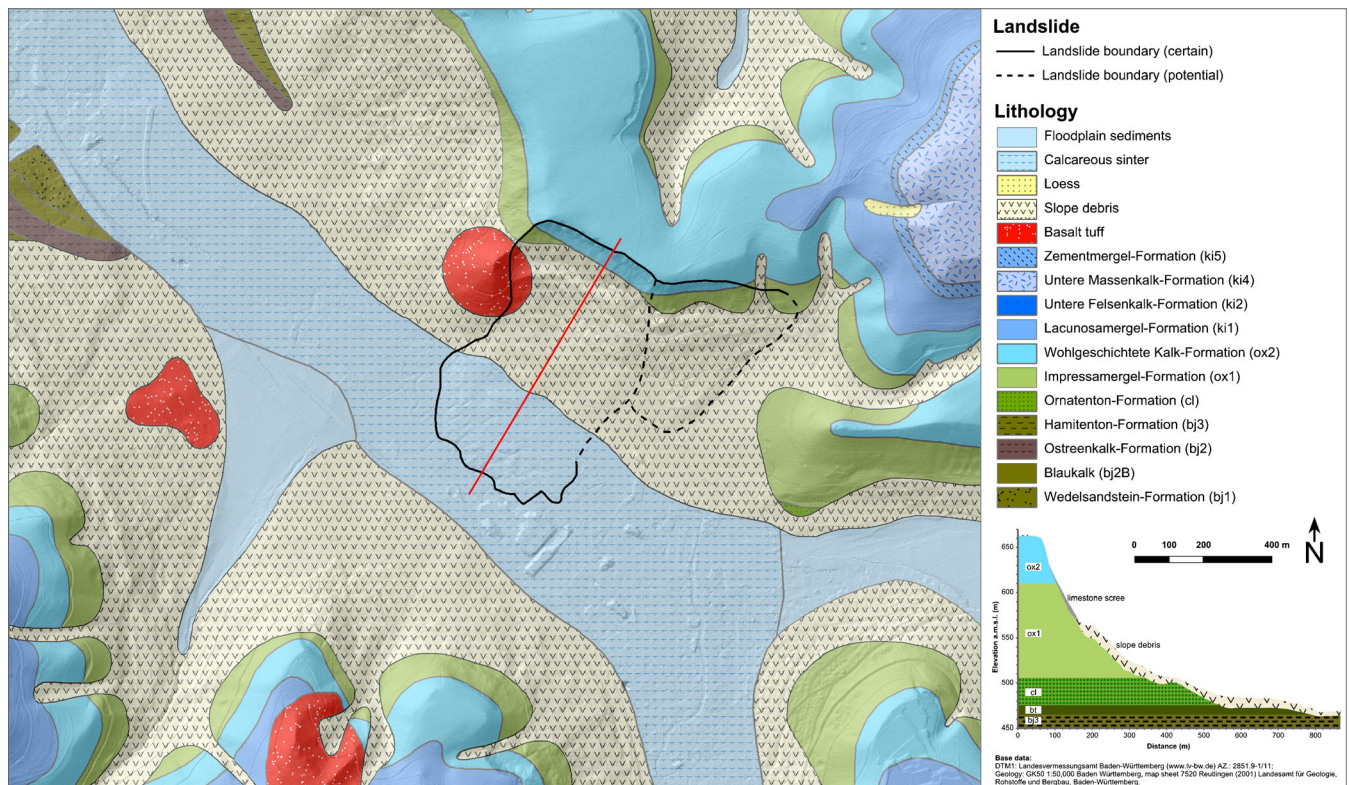


Fig. 2 Geology map of Lichtenstein-Unterhausen (after Bell 2007). The red line indicates the position of the cross profile presented in the lower right corner. Note that the cross profile is based on results described below and includes two classes not presented in the geology map itself, i.e. the limestone scree on the upper slope and the Dentalienton (bt) which was described by Ohmert et al. (1988)

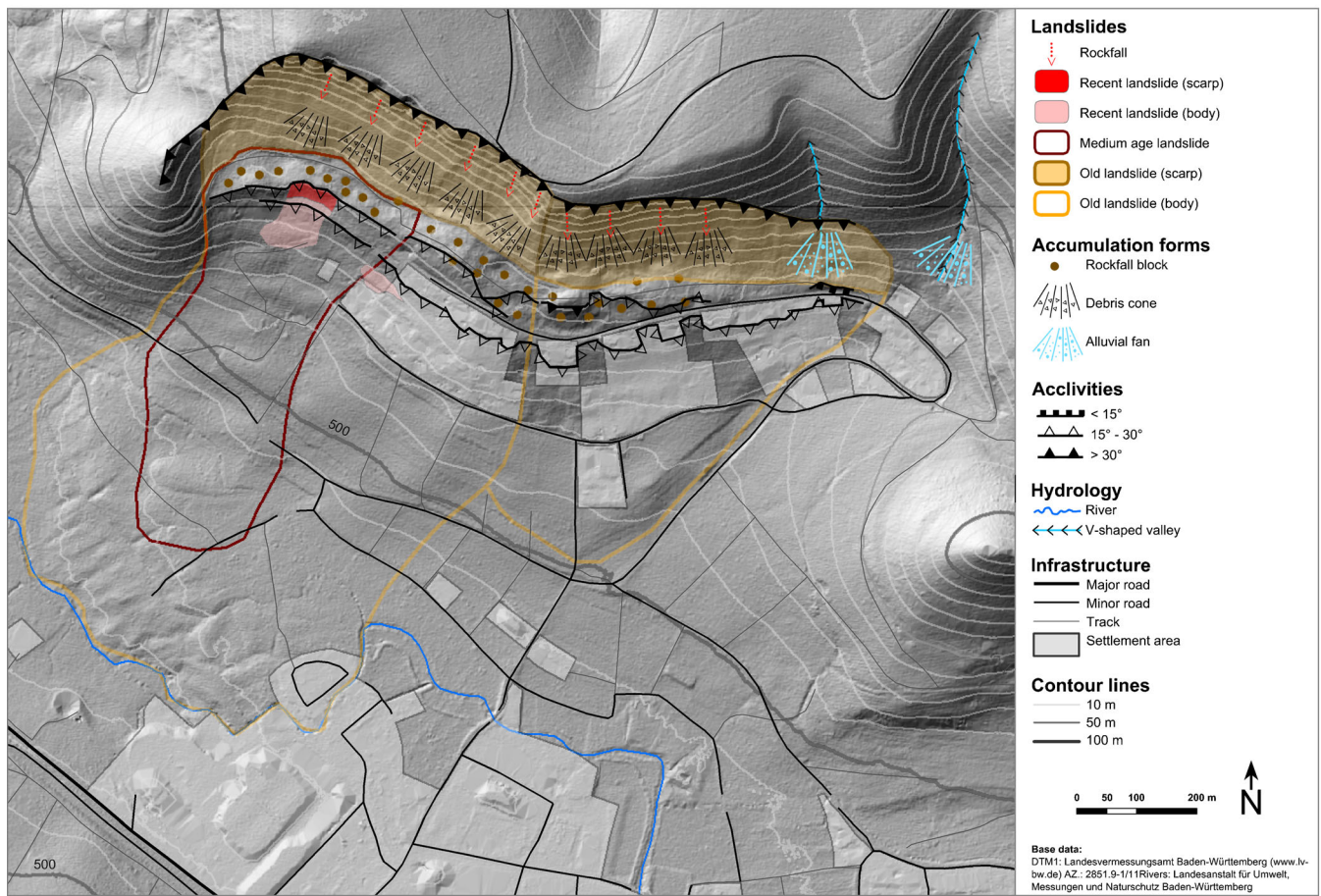


Fig. 3 Geomorphological map of Lichtenstein-Unterhausen (after Bell 2007)

Superficial and shallow landslide activity can be observed on all slope areas without settlement. A highly active scree slope, formed of loose limestone, is located above the head of the oldest landslide deposit. Limestone rocks originating from the ox2 limestone stratum in the landslide head scarp areas spread out at the foot of the scree slope, indicating high rockfall activity. The limestone was earlier mined, and an overall volume of approximately 30,000 m³ extracted (Schönwälder 2006 in Bell 2007).

Previous landslide investigations

The study area Lichtenstein-Unterhausen has been subject to landslide-related investigations since 2003 (Bell 2007; Bell et al. 2006; Sass et al. 2008). An initial landslide monitoring system was installed comprising inclinometers, geodetic levelling and temporary tiltmeter measurements (Bell 2007). Based on the monitoring data, it was concluded that at least parts of the landslide are seasonally reactivating, leading to extremely slow downslope displacement rates of approximately 2–3 mm per year. Two distinct patterns of movement were distinguished: a deep-seated sliding process down to the bedrock occurring in spring, and a flow movement in summer and autumn. Herein, flow refers to a continuous movement with a distribution of velocities similar to viscous liquid (Cruden and Varnes 1996; Dikau et al. 1996). The onset of the shallow displacements was found to

coincide with structural damage at one house, where cracks in the outer walls widened. An analysis of landslide movements and rainfall data showed no evident correlation. However, a causal relation between snow melting and deep-seated sliding could be established based on the timing of displacements, and the absence of deep-seated sliding during years of little or snow melting (Bell 2007). More extensive interpretations of landslide behaviour were limited by lack of detailed climatic data, the small spatial extent and short time period of the slope monitoring, and extremely slow movement rates, close to the instruments' margin of error. Four monthly geoelectrical surveys were carried out by Kruse (2006). One of the main results of that investigation was that the limestone scree allows for rapid infiltration of rainfall and melting snow, possibly an important factor for initiation of landslide movement. It was, however, not possible to establish a relationship between geoelectrical monitoring data and landslide displacement, nor to detail the subsurface hydrological processes.

Between 2007 and 2008, the existing slope monitoring system was extended by the ILEWS project (Integrative Landslide Early Warning Systems) (Bell et al. 2010a) (Fig. 4). Two additional inclinometers were installed (Lico4 and Lico5) and one automated in-place inclinometer chain was put into the existing borehole Lico2. Furthermore, regular surface movement monitoring was carried out by total

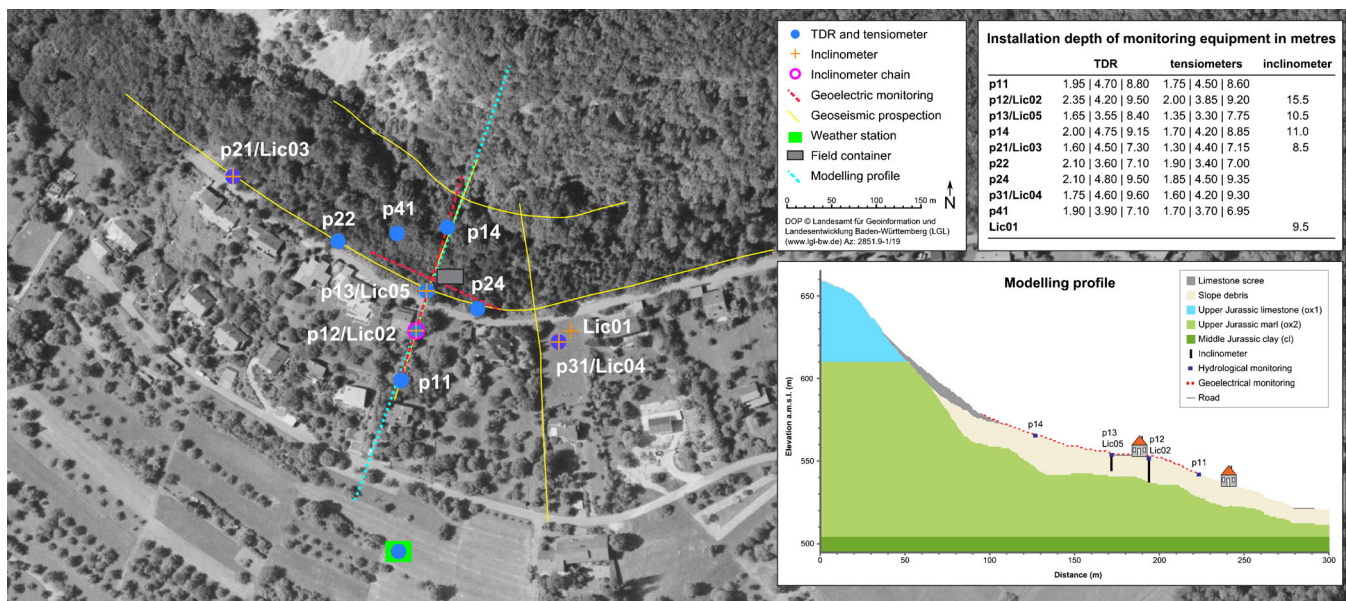


Fig. 4 Monitoring system, installations and subsurface conditions along the profile used for modelling

station measurements every 3 months on 15 fixed points (Aslan et al. 2010). An extensive hydrological monitoring system, comprising TDR sensors and tensiometers located in three depths between 2 and 10 m at nine different locations, was installed to take continuous measurement of soil suction, pore water pressure and volumetric water content (Camek et al. 2010). Additionally, two geoelectric resistivity profiles were installed to improve the understanding of subsurface hydrological processes (Wiebe and Krummel 2010). Detailed investigations of slope hydrology and the relation to landslide displacements are provided by Wiebe et al. (2010) and Thiebes (2012; 2011), respectively.

The main landslide-related findings of the ILEWS project can be summarised as:

- the previously assessed extremely slow slope movements continued until today and amount to approximately 1.5 cm in 6.5 years (Fig. 5). The shallow displacements at approximately 8.5 m depth, initially described as flow-like (Bell 2007), from the most recent measurements show signs of a transition to a sliding movement process, which can be interpreted as a development of a discrete shear surface;
- slope hydrology is of major importance for the reactivation of slope movements. Deep-seated sliding can be observed after spring snow melt, while the shallow displacements primarily occur after major rainfall events. Infiltration and subsurface water flow varies for different locations and preferential paths allow for rapid propagation of water to significant depths;
- in some monitoring positions, the extremely slow displacement rates are still within the margin of error of the monitoring equipment, and it is not possible to determine clear hydrological thresholds of landslide reactivations. Based on current monitoring data, it is not possible to determine the boundaries of current reactivations; however, the general displacement trend is clearly detectable and causes ongoing damage to existing infrastructure.

- an acceleration of slope movements could have dramatic consequences, with a maximum loss of private property of EUR 18.5 million (US\$ 25 million) in addition to EUR 1.7 million (US\$ 2.3 million) damage to communal infrastructure (Greiving 2010).

Methods

The methodological approach pursued in this study consists of two major steps: the application of a limit-equilibrium slope stability model to the landslide in Lichtenstein-Unterhausen and the subsequent implementation of the model into a prototypic early warning system.

Landslide modelling

Combined Hydrology and Stability Model (CHASM)

For the assessment of slope stability and early warning modelling, the physically based landslide simulation model CHASM was used, which combines the simulation of saturated and unsaturated hydrological processes to calculate pore-water pressures, which are then incorporated into the computation of slope stability by means of limit-equilibrium analysis. The CHASM model has been applied under various environmental conditions, for example in New Zealand (Wilkinson et al. 2000), Malaysia (Collison and Anderson 1996; Lateh et al. 2008), Hong Kong (Wilkinson et al. 2002a), the Caribbean (Anderson et al. 2008), Kuala Lumpur (Wilkinson et al. 2002b; Wilkinson et al. 2000) and Greece (Ferentinou et al. 2006; Matziaris et al. 2005; Sakellariou et al. 2006). Below, a brief review of CHASM is presented; however, it is beyond the scope of this paper to describe all features and the underlying constitutive equations, which can be found elsewhere (e.g. Anderson et al. 1996; Anderson and Richards 1987; Anderson and Thallapally 1996; Collison and Anderson 1996; Wilkinson et al. 2002a; Wilkinson et al. 2000).

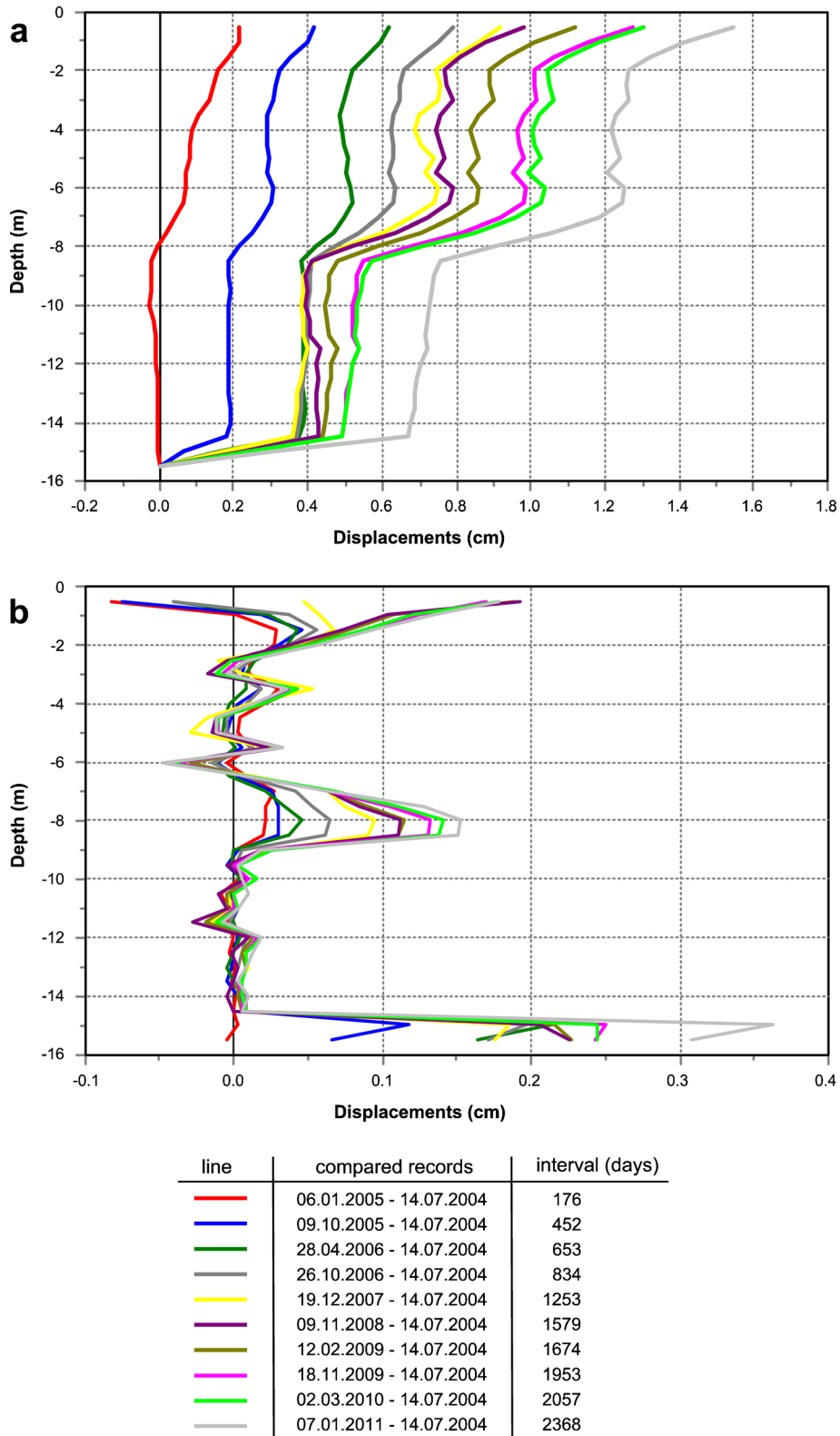


Fig. 5 Downslope displacements measured by manual inclinometer at borehole Lic02; integrative plot (a) and differential plot (b)

The procedure for hydrological modelling adopted in CHASM is a forward explicit finite difference scheme (Wilkinson et al. 2002b). The slope is divided into a series of columns of which

each is subdivided into regular cells. Detention storage, infiltration, evapotranspiration, and unsaturated and saturated flow regimes are modelled within CHASM. Infiltration into the soil is

determined by the infiltration capacity of the top cell, being a function of hydraulic conductivity and the prevailing pore water pressure. Additionally, a surface detention capacity is included and is the maximum ponding depth of water allowed on the slope surface before surface runoff is generated (Wilkinson et al. 2002b). Ponding occurs when the precipitation rate exceeds the hydraulic conductivity of the top cell and is accommodated within the predefined detention capacity. If the detention capacity is exceeded during a storm event, any resultant surface runoff is routed to the next adjoining downslope surface cell for potential infiltration into the slope. Unsaturated vertical flow within each column is computed using Richards equation (Richards 1931). Unsaturated conductivity is defined by the Millington and Quirk (1959) procedure. Flow between columns is simulated by Darcy's equation for saturated flow, adopting the Dupuit–Forchheimer (Forchheimer 1930) assumption. Numerical stability of the solution to the Richards equation depends on the simulation time step and applies a methodology proposed by Beven (1985) in which the required time step (iteration period) is based on the distance between the computational nodes, the gradient of the suction–moisture curve at a given suction value and the flow velocity. For most applications, the recommended spatial resolution is an individual cell size of 1 m (Wilkinson et al. 2002a, b). Slope curvature (convexity and concavity) can be integrated by adjusting the column breadth to represent, and investigate, the effects of three-dimensional topography on pore water pressure. Simulated pore water pressures are incorporated into the effective stress determination using the Mohr–Coulomb equation for soil shear strength, following Bishop's simplified circular method (Bishop 1955) or Janbu's non-circular method (Janbu 1954) method. For each hour of the simulation, a minimum Factor of Safety (FoS) is computed, temporal variations of which arise on account of hydrodynamic responses and the consequential changes in the position of the critical slip surface. Moreover, vegetation and certain stabilisation measures can be integrated into the stabilisation analysis.

Input data requirements

To apply CHASM to the study area, it was essential to prepare the required input data which includes a slope model describing the material layers in the subsurface and their geotechnical characteristics, groundwater conditions, rainfall scenarios and the definition of shear surface search parameters.

The slope model used for CHASM simulation was compiled from a range of data sources, including geological maps, drillings and geophysical surveys. Four material types were identified and accounted for in slope stability modelling with CHASM, i.e. Upper Jurassic limestone, Middle Jurassic marl, the limestone scree present in the head scarp area of the large landslide body and the superficial regolith (slope debris) covering most of the study area. Accurate determination of material boundaries in such circumstances is complex. However, we took what we consider to be a holistic approach; researching and acquiring known pre-existing site data, supplemented with on-site determinations to deliver a slope representation deemed adequate for the purpose of formulating an initial early warning methodology. In that process, we recognised the issues of geological, hydrogeological and human uncertainties (i.e. errors or misjudgement in respect of landslide

risk management), accepting that 'the use of imperfect knowledge based on limited information is guided by judgement and experience in the formulation of geological models and characterization of the engineering properties' (Ho and Lau 2010). The upper and lower limits of the Upper and Middle Jurassic were extracted from the geological map (1:50,000), neglecting the small tilt of these lithological units. The spatial extent of the limestone scree slope was mapped on a digital orthophoto. The thickness of the limestone scree was determined from the geoelectric resistivity measurements by Kruse (2006) who extended his profile relatively far upslope. For the uppermost sections, for which no depth information was available, a gradually decreasing scree thickness was assumed. The estimation of the thickness of slope debris was based on the seismic refraction prospecting carried out by Bell et al. (2010b)). Even though a total of five drillings of moderate depths (8–16 m) had been performed along the selected slope profile, only borehole Lico2 reached the bedrock. It was assumed that the seismic characteristics at this location were representative of the rest of the selected profile. Finally, all information on the subsurface materials was combined to a slope model with a 1-m resolution.

Geotechnical parameters required for CHASM simulations include effective angle of internal friction, effective cohesion, hydraulic conductivity, saturated and unsaturated bulk density, saturated moisture content and suction moisture curves. Laboratory analyses of samples taken in the field provided information on soil particle distribution, but were not sufficient for the parameterisation of CHASM. Cohesion and internal friction were determined based on a database of geotechnical parameter values from experimental analysis collected from various literature sources (Meyenfeld 2010, personal communication). Hydraulic conductivity (K_{sat}) values were estimated from standard values available in Bear (1972) and DIN standard (DIN 18130). Hydraulic conductivity of the slope debris as well as the suction moisture curves and saturated moisture content were assessed based on soil particle size distributions by the SPAW model (Soil–Plant–Air–Water) (Saxton and Rawls 2006; Saxton and Willey 2006; Sung and Iba 2010). The geotechnical parameters were tested in CHASM and adjusted to reflect known field conditions and behaviours, as discussed more fully below. A back-analysis of the previous slope failures, such as the artificially caused landslide in 1985, could not be carried out because the exact conditions of the failures are unknown.

Groundwater conditions were derived by an analysis of hydrological monitoring data. The determination of the annual minimum and maximum groundwater positions was made using tensiometer measurements, which provide relative water table height if they are located below the groundwater table. Measured positive pressures were related to relative water table heights by the conversion $100 \text{ hPa} = 102.15 \text{ cm}$ stated by the sensor manufacturer (UMS 2007).

Rainfall scenarios used in the study were based on the KOSTRA atlas (Bartels et al. 2005; Malitz 2005) developed by the German Weather Service (DWD). KOSTRA is based on a complex statistical regionalisation of precipitation data between 1951 and 2000 using 4,500 climate stations in Germany, and provides rainfall intensities for event durations between 5 min and 72 h, as well as annual occurrence probabilities from 0.5 to 100 years.

Slope stability assessment

In this study, the command-line version of CHASM (v4.12.5) was used for slope stability analysis and early warning modelling. Shear surfaces were calculated using Bishop's methodology for circular shear surfaces. The effects of vegetation and three-dimensional topography on slope stability were neglected in this study, and the respective CHASM extensions were not used. The analysis of CHASM results concentrated on the FoS as the prime output of slope stability simulations; the temporal development of the FoS, as a response to rainfall, and the associated hydrological processes were analysed.

Slope stability simulations using CHASM were carried out to investigate the characteristics of a partial reactivation of the existing landslide body. This included the calculation of likely shear surfaces and an assessment of the influence of rainfall and groundwater conditions on slope stability. Slope stability simulations focused on one specific slope profile (see Fig. 4), for which slope movements and related infrastructure damage had been confirmed by previous investigations, and for which hydrological monitoring data were available.

Early warning

The main tasks for an integration of CHASM into a landslide early warning system comprise the automation of CHASM to calculate the slope stability according to quantitative rainfall forecasts, the visualisation of the respective modelling results and the automated notification according to a well-planned chain of communication.

A complex data management and visualisation platform was configured complying with the standards of the Open Geospatial Consortium (OGC) to ensure the interoperability of the system. The main goal of the web-based application is to visualise monitoring data and modelling results, and to provide relevant experts with notification on the current status. It is beyond the scope of this paper to describe the technical implementation in detail; this is available elsewhere (Jäger et al. 2010, 2012). In this paper, only two applications will be highlighted, which are important for early warning. The first is the CHASM web processing service (WPS), which essentially runs the CHASM algorithm on a server; the second is the web notification service (WNS), which automatically sends SMS and email messages to experts, when pre-defined alarm thresholds are exceeded. Whereas some of the OGC standards have been already successfully integrated into geologic and landslide research projects, in particular web mapping services (WMS), WNS and WPS have rarely been described (e.g. Cannata et al. 2010). In case of the WPS, the OGC specifications define a standardised interface for offering processing capabilities within a geospatial data infrastructure. However, these do not limit the processing capabilities to familiar, standard, GIS operations such as polygon intersection, but allow for complex process models such as CHASM to be offered. In this study, CHASM was implemented as a WPS according to the specifications of version 1.0.0 (Schut 2007). The WNS utilised the implementation by 52North (<http://52north.org/>), which works as a Tomcat web application. The specifications are provided by Simonis and Echterhoff (2006). Both the WPS and WNS services were implemented as Java web applications with a qooxdoo-AJAX frontend (<http://qooxdoo.org/>).

In order to meet the demands of the local and regional decision-makers responsible for landslide risk management, the implementation of the early warning system was planned in cooperation with

the relevant agencies (Mayer and Pohl, 2010). Meetings were held to discuss and determine the expectations and demands of involved stakeholders such as the local government, the administrative office for civil protection, the district office and the federal geological survey. Topics considered during these meetings focused on the respective preferences for the provision of information on 'current' monitoring, and early warning status, and the chain of communication when potentially threatening developments can be anticipated.

Results

Landslide modelling

Input data generation

The assessment of slope stability, and subsequent modelling of early warning scenarios, primarily focused on a slope profile on the main western landslide body with a total length of 300 m and a slope height of 165 m. This profile coincides with the western longitudinal seismic profile and the longitudinal geoelectric profile (see Fig. 4), but extends further up- and downslope. The highest point is on the relatively flat plateau, the lower-most extent is below the lower road. Four hydrological monitoring points (p11–p14) and two inclinometers (Lico2 and Lico4) have been installed along this profile.

Based on the geological maps (1:50,000), the boundary between Upper and Middle Jurassic was assessed to be at 505 m a.m.s.l. The limestone scree in the upper section of the selected profile was assessed to have a maximum thickness of approximately 8 m. It was assumed that the scree slope had developed after the initial landslide event, and the scree material therefore only covers the surface and is not buried below the slope debris. Approximately 170 m of the profile, for which modelling of slope stability and early warning was focused on, were covered by two seismic refraction measurements (Fig. 6). At inclinometer Lico2, where the bedrock was confirmed by drilling; the measured wave velocity was approximately 2,000 m/s, which was subsequently used for the rest of the assessed profile. The resulting depths of slope debris varied between 13 m and 16 m for most parts of the profile; however, at some locations depths of more than 20 m were estimated. A refractor, computed using the plus-minus method, was calculated around 900 m/s, relating to a depth between 6 m and 8 m. Bell et al. (2010b) interpreted the refractor as a weak zone. At this depth, large limestone boulders were found in some drillings; however, no geomorphologically viable explanation could be found to justify the assumption that this is the case for the entire profile. Consequently, the refractor was not considered further. The selection of appropriate geotechnical parameters of necessity includes significant expert judgement; Muir-Wood D et al. (1993, p 510) comment on 'the need for the user to ensure that the parameters that are chosen are indeed reasonable'. Moreover, the optimum model selection cannot be determined by fitting to a single test or back-analysis (Muir-Wood 2004), and more broadly Konikow and Bredehoff (1992) stress that models cannot be 'validated', but only tested or invalidated. In accord with these views, geotechnical parameters were chosen using a priori information (Table 1) and the resultant model behaviour tested to ensure the physical consistency of the within-model behaviour, consistency with process behaviours inferred from observations, and known slope behaviour (Thiebes 2011, 2012). The

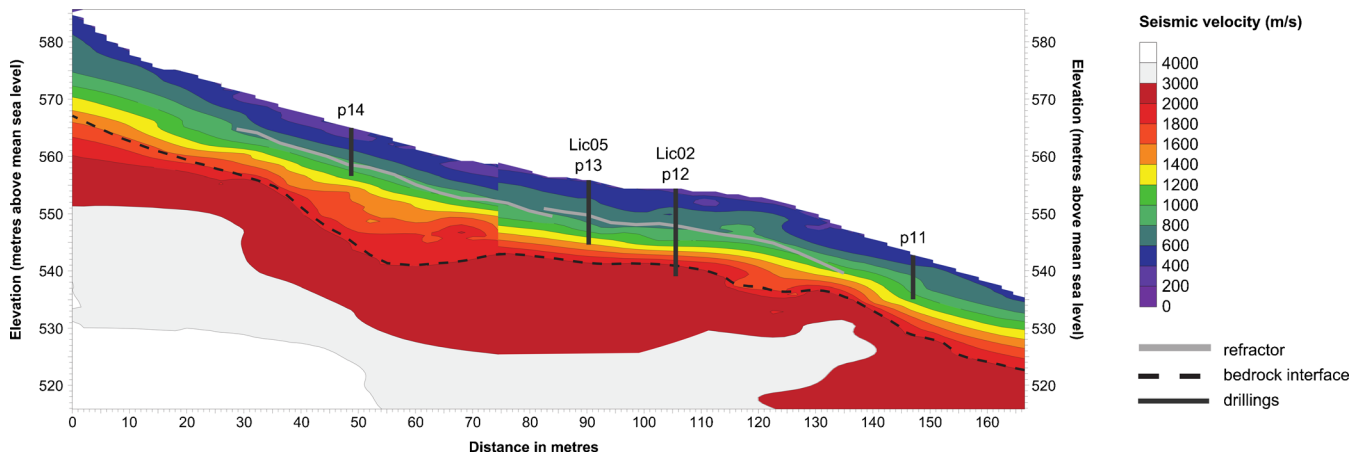


Fig. 6 Seismic refraction analysis and estimated bedrock interface

limestone scree can be characterised by high hydraulic conductivity and low effective cohesion. Parameterisation of the slope debris was more difficult due to the complex subsurface field conditions. Drillings and subsurface investigations by a borehole camera revealed a strongly varying subsurface material composition; very dense clay, and marl layers intersected by sections of limestone blocks which frequently collapsed into the borehole during drilling. Laboratory analyses of the sieved fine material indicated the soil type as mostly silty clay and clay loam, according to the US texture classification. Clay content was as high as 54 %, and 38 % on average, while sand content was determined to be generally below 1 %. The geotechnical values for the slope debris material were therefore chosen to be intermediate for internal friction, effective cohesion and hydraulic conductivity. The determination of geotechnical parameters for the Upper and Middle Jurassic had to be largely based on subjective estimation due to the lack of field samples. For the Upper Jurassic, medium values for internal friction and effective cohesion were selected to allow CHASM to focus on reactivations of the slope debris sliding along the more stable bedrock. For the Middle Jurassic located below, more stable (higher shear resistance) geotechnical parameter settings were selected. However, this material layer did not play an important role in this study since the objective was to assess conditions leading to a reactivation of the previously moved landslide material.

The hydrological monitoring data available from a series of tensiometers and TDR sensors were analysed to determine groundwater elevations for subsequent modelling. Overall, the hydrological data showed a clear annual variation, with higher soil moisture and

groundwater elevations in winter and spring, and drier conditions during summer and autumn. Most sensors installed at relatively shallow depths reacted quicker to larger rainfall and snow melting events than sensors installed at greater depths. The deepest tensiometers exhibited saturation (and positive pore water pressures) over long periods. However, at some locations marked responses to rainfall and snow-melting events could be observed for the deepest sensors, interpreted as evidence of the existence of preferential flow paths.

The determination of minimum and maximum groundwater elevations mainly utilised the shallow and medium depth tensiometers which were saturated or measured positive pore water pressure for some time of the year. The resulting groundwater table depths varied between 1.3 m and 2 m for the wet periods, and 3.7 m and 6 m during drier phases. The spatially interpolated groundwater elevations are illustrated in Fig. 7.

Application of CHASM

Several potential shear surface positions were investigated within this study for which the FoS varies depending on the initial groundwater conditions and rainfall scenarios. Figure 8 displays the minimum FoS for a selection of tested slip surfaces using the maximum groundwater elevations, combined with a 5-h design rainfall event with an intensity of 10 mm h^{-1} having a probability of occurrence of approximately one in 50 years.

The lowest minimum FoS of 0.75 was assessed for the uppermost shear surface (green) which relates to a slope failure of the lower parts

Table 1 Selection of geotechnical properties estimated for the material layers used in CHASM simulations

Parameter	Unit	Upper Jurassic	Middle Jurassic	Slope debris	Limestone scree
Effective cohesion	kN m^{-2}	300	1,500	19	0
Internal friction	$^{\circ}$	35	15	20	33
Hydraulic conductivity (K_{sat})	m s^{-1}	10^{-6}	10^{-9}	6.78^{-7}	10^{-1}
Moisture content (sat)	$\text{m}^3 \text{ m}^{-3}$	40.7	44.7	52.6	48.3
Bulk density (sat)	kN m^{-3}	25	23	16	16
Bulk density (unsat)	kN m^{-3}	23	21	15	15

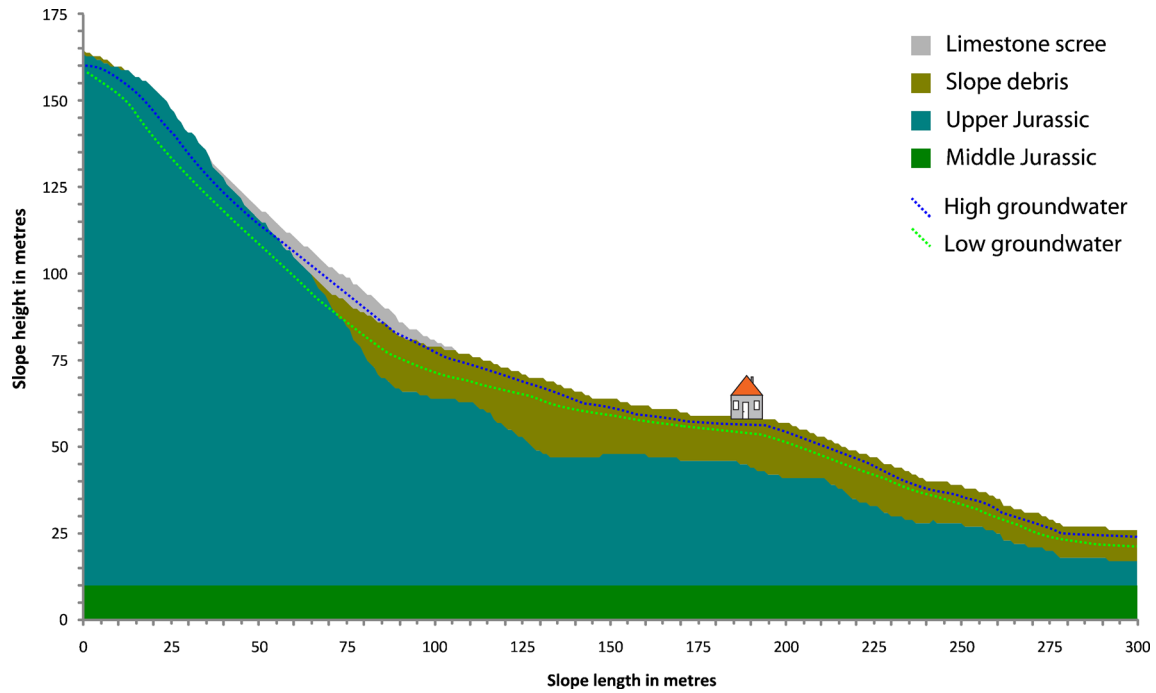


Fig. 7 High and low groundwater scenarios

of the limestone scree slope and the slope debris. However, there is no field evidence supporting instability in this area. A likely reason for this disparity is the inherent difficulty of representing the field complexity of the interface between the three constituent materials of limestone scree, Upper Jurassic and slope debris, in the vicinity of the

upper part of the predicted slip surface. A slightly larger potential reactivation located further downslope (pink) resulted in a minimum FoS of 1.4. The largest potential partial landslide reactivation modelled includes only the slope debris. The respective shear surface (yellow) has a minimum FoS is 1.05 and affects the damaged house at

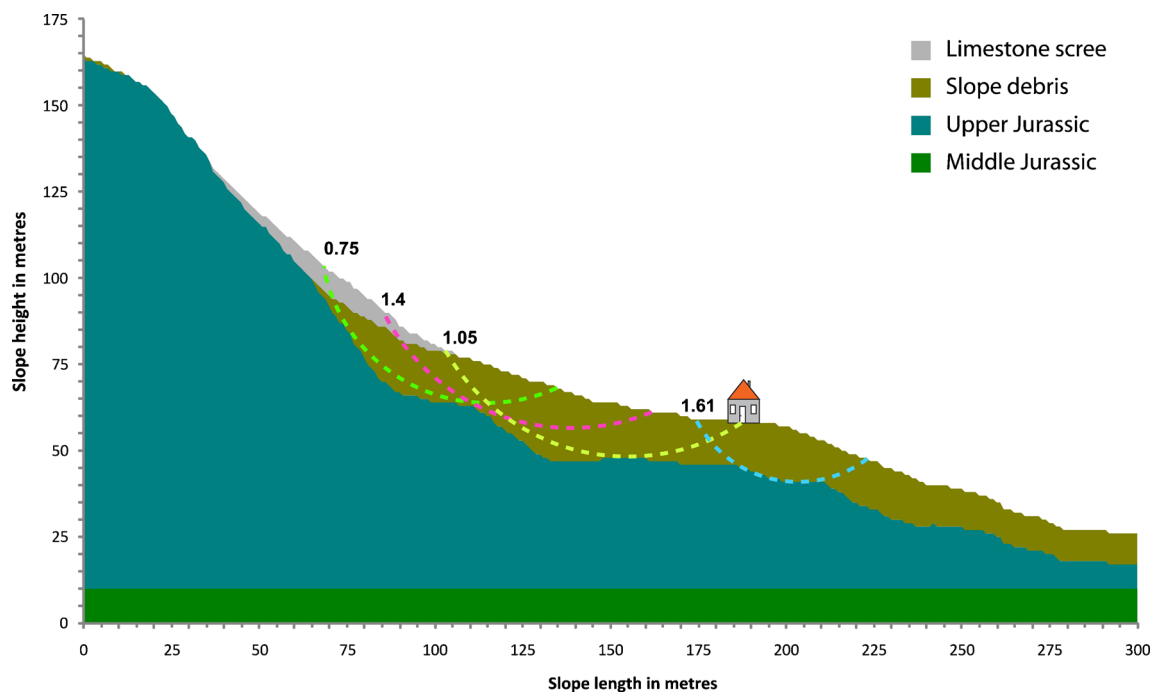


Fig. 8 Calculated shear surfaces and respective minimum FoS for high groundwater conditions and a 5-h design rainfall of 50 mm in total

its lower end. This shear surface was assumed to be the most realistic and consequently used for early warning. The highest FoS was calculated for the potential shear surface (cyan) located below the damaged house, for which the minimum FoS was 1.61. Other shear surfaces not displayed here were also tested, including failures comprising bedrock. However, the FoS for such shear surfaces were significantly higher, with values between 3.0 and 6.0.

CHASM simulations utilising the lower groundwater scenario resulted in more stable conditions, with FoS between 0.03 and 0.17 higher at the end of the simulation, with rainfall intensity having a limited influence on the modelled FoS. The difference between the predicted FoS for a one-in-1-year 24-h rainfall event (38.4 mm) and a one-in-100 years 'worst case' rainfall event (120 mm) was assessed to be as low as 0.1. Using the selected model configurations, no FoS below 1.0 was simulated using individual rainfall events, even with high intensity. Lower-than-unity FoS values could only be achieved following consecutive rainfall events or by increasing the rainfall intensity five- to tenfold. Figure 9 illustrates the CHASM results for a model run for minimum and maximum groundwater conditions, and two consecutive rainfall events, a 24-h rainfall (one-in-100-year occurrence probability), followed by a 6-h 'worst-case' scenario rainfall (one-in-100-year occurrence probability). In both model runs, the FoS decreases until the first rainfall event commences in hour 10 of the simulation. This trend continues for the low groundwater scenario until the end of the simulation period, with an eventual stabilised minimum FoS of ~1.09. For high water conditions, the FoS recovers after the first rainfall, and then decreases during the second event, reaching a minimum of 0.99 some 12 h after the cessation of precipitation.

Early warning

The automation of slope stability calculations with CHASM was implemented as a WPS. This server-based simulation is used to forecast slope conditions based on fixed and variable input data. Automated notifications are automatically issued if the FoS falls below a pre-defined threshold. An overview of the modelling procedure is presented in Fig. 10.

Fixed input data were chosen according to the results of previous conventional CHASM modelling and include the slope profile, the shear surface parameters and soil characteristics. For early warning modelling, the profile along the damaged house on which previous modelling focused on was used. The fixed shear surface parameters relate to a potential failure in the upper slope area which affects the damaged house at the lower end.

Variable data include recorded precipitation, rainfall forecasts and groundwater conditions. Measured rainfall from the local weather station and forecasted precipitation from COSMO-DE simulations (Consortium for Small Scale Modeling 2007) are combined into one rainfall file computable by CHASM. COSMO-DE is the complex weather forecasting model employed by DWD for short-term prediction of weather conditions (Deutscher Wetterdienst 2010a, b) and has a spatial resolution of 0.025° (2.8 km × 2.8 km grid cells). COSMO-DE is the German contribution to the Consortium for Small-Scale Modeling (COSMO). The model simulates meteorological processes and predicts parameters such as air pressure, temperature, wind, water vapour, clouds and precipitation with the aim to provide timely warning for severe weather conditions (Consortium for Small Scale Modeling 2007). Quantitative rainfall forecast from COSMO-DE model were provided by the DWD for the period from September 2006 to December 2009 as cumulative simulation runs.

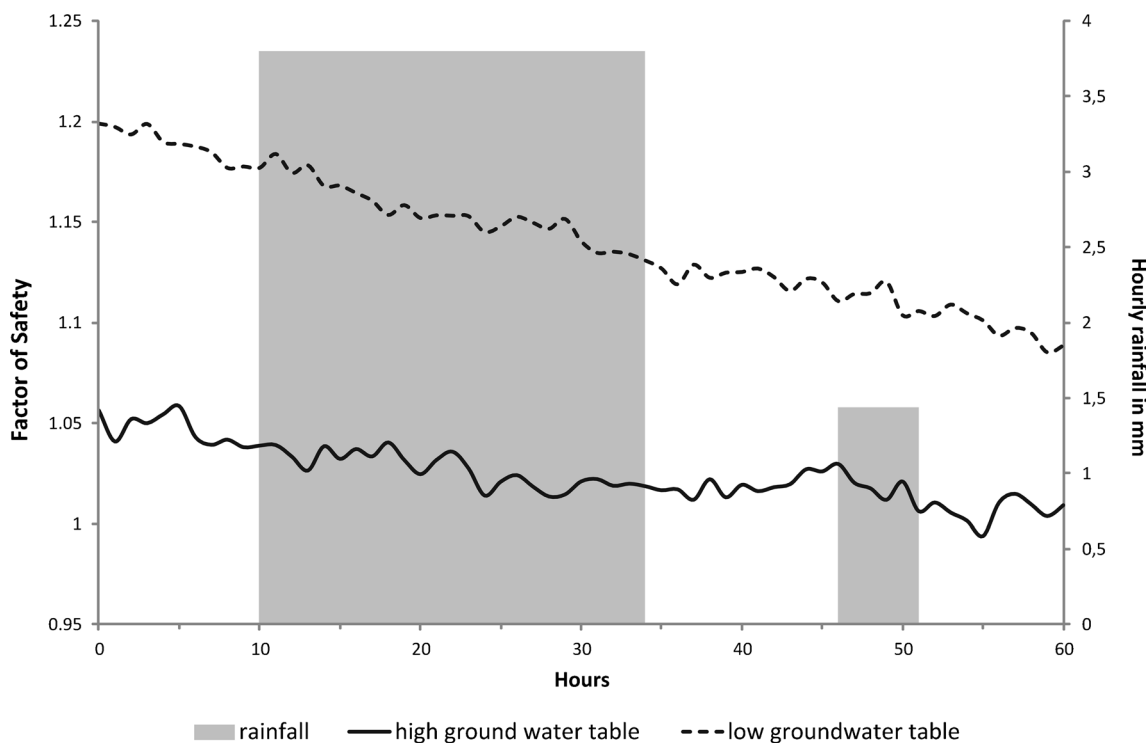


Fig. 9 Factor of Safety development during successive rainfall events

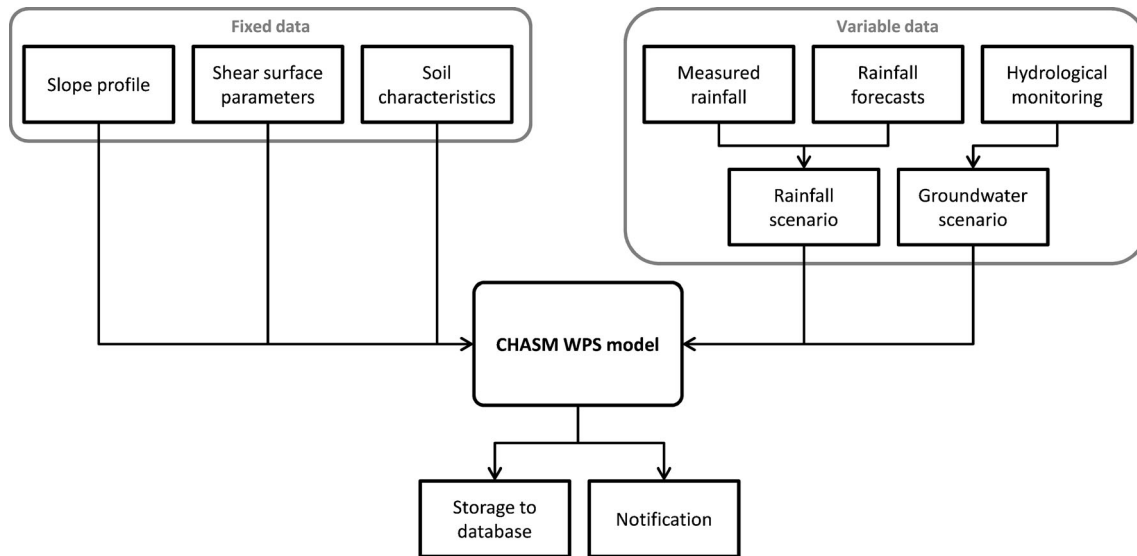


Fig. 10 Flowchart of the CHASM WPS model

For every day, two simulations, each with a simulated length of 12 h, were available in GRIB format.

Groundwater scenarios are chosen depending on current hydrological conditions recorded by the monitoring system. For this, a TDR sensor in 9.5 m depth located at the damaged house (monitoring site p12) was selected because it reacts quicker and more reliable to groundwater changes than the nearby tensiometers. In the current settings, a threshold of 40 % volumetric water content was taken because this value corresponds to the conditions described in the high groundwater scenario. If measured soil moisture is higher than the thresholds value, the high groundwater table scenario is chosen; a lower soil water content results in the integration of the low groundwater table scenario.

Fixed and variable input data are both integrated into the server-based CHASM WPS model which automatically initiates the simulation every 24 h. In the current setting, this file comprises a total simulation length of 60 h and includes 30 h of recorded rainfall, 20 h of forecasted rainfall and 10 h without any precipitation. The last 10 h without precipitation were included because it was found that the lowest FoS does not necessarily coincide with peak rainfall, but can also occur shortly after due to the time needed for rainfall to infiltrate.

The results of the model runs are stored in a database for later access, and a notification is sent to the involved experts if a specified FoS is not reached. The status of slope monitoring system and CHASM WPS simulations can be viewed online.

A screenshot of the implemented data management and visualisation platform is presented in Fig. 11. Artificial alert thresholds (a) are implemented for all physical sensors in the field that provide continuous monitoring data. The alert thresholds refer to changes of the measured parameter values over different periods of time, e.g. a change of pore water pressure or inclination within the last 2, 6, 12 and 24 h. The latest measurements are compared to the predefined threshold values and displayed as an alert level (b) in percent. The most recent changes of the measured parameter values can also be illustrated as a graph over time. An additional alert threshold is implemented for the results of the

CHASM WPS model where the threshold value refers to the minimum FoS of the simulation. Moreover, alert thresholds for the forecasted precipitation are implemented and thereby accommodate regional rainfall thresholds. However, it should be noted that only historic rainfall forecasts were available for this study, and no realistic early warnings can be issued. Consequently, the alert thresholds relating to forecasted precipitation and to the results of the CHASM WPS are currently deactivated. In addition, the current status of all alert thresholds are visualised as alert sensors (c), which change from green to yellow if the respective pre-defined threshold values are exceeded. At the same time, automated messages are sent by the WNS to a list of subscribers. Ultimately, these alert thresholds influence the three-coloured early warning signal (d), which is used to communicate the current warning status and hazard situation. An overview on the operating mode of the early warning signal is presented in Fig. 12.

As long as real-time measurements are below the pre-defined alert thresholds, the warning signal is on green, indicating that no critical situation is expected. Once a threshold value is exceeded, the respective alert signal, as well as the warning signal, changes to yellow to indicate an unusual situation. Simultaneously, SMS and emails are sent to experts and registered users (e.g. local and regional administration) to inform them that a pre-defined monitoring, or modelling, threshold has been exceeded. The experts are requested to interpret the outputs and decide whether the situation is potentially dangerous or a possible false alarm. Depending on the experts' decision, the warning signal light is either re-set to green or upgraded to red. Subsequently, subscribers are notified about the updated warning level and the reason for the experts' decision. Additionally, a red warning status is directly followed by automated messages with action advisories to registered users, and emergency services. The highest (red) warning level cannot be issued automatically by the system, but only by an authorized operator with editing rights, thereby, it is hoped, minimising false alarms.

In this study, the local administration, whilst having comparatively little interest in detailed visualisation of monitoring data and

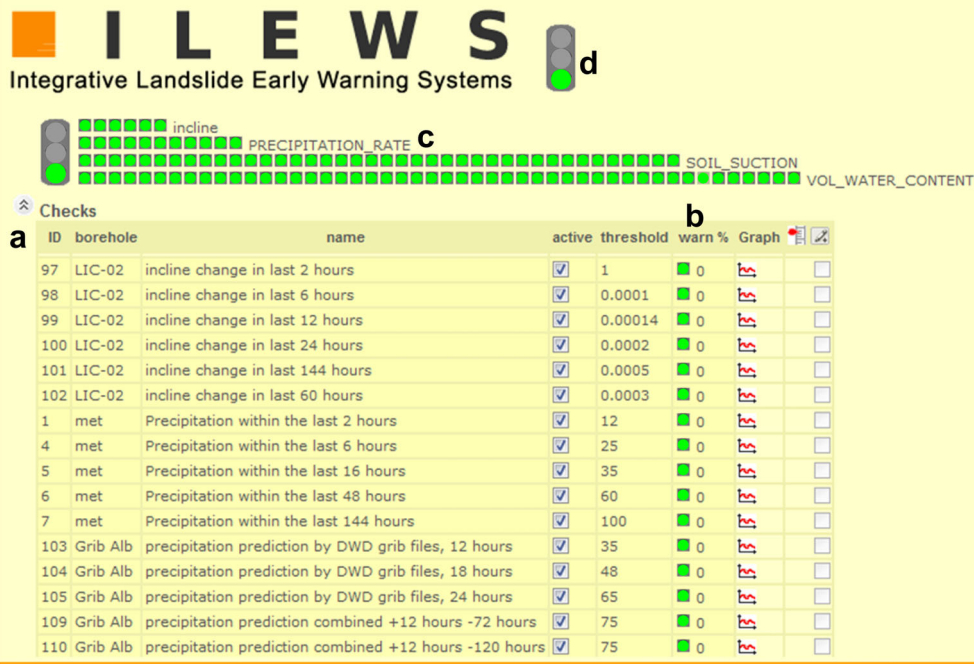


Fig. 11 Screenshot of the ILEWS status control and warning platform with alert thresholds (a), alert levels (b), alert sensors(c) and early warning signal (d)

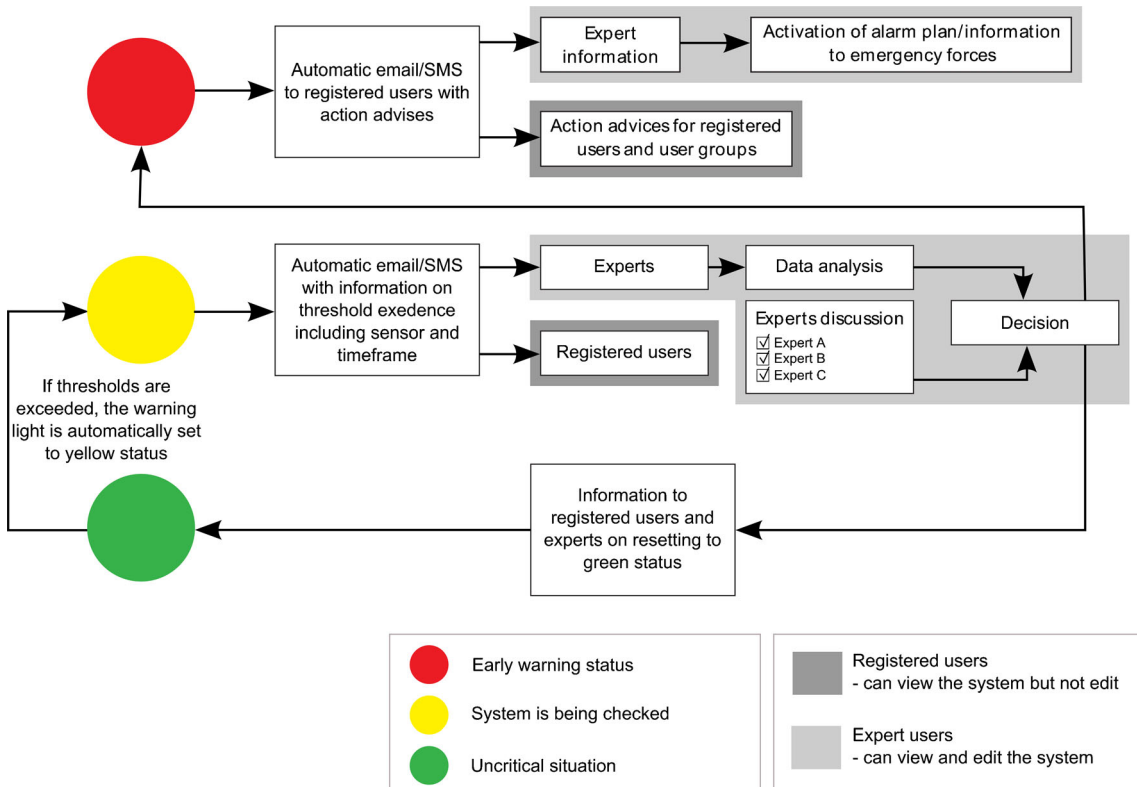


Fig. 12 Early warning procedure (after Mayer and Pohl 2010)

other scientific products, had been interest in the notice required if emergency actions have to be initiated. Consequently, the local administration was provided only with 'viewing' permission to the system.

Regional-level authorities responsible for hazard management and civil protection, such as the district office (Landratsamt) and regional councils (Regierungspräsidien) were also asked for their requirements regarding an early warning system. The contacted agencies showed a good understanding of the problems related to landslide occurrence in the region and appreciated the scientific work reported here. However, none of the regional stakeholders wanted to act as the 'expert' responsible for the early warning system prototype. These reasons for this are twofold. First, the very low movement rates of the landslide itself do not present an imminent danger; and second, the legal responsibility for early warning systems is not clearly defined in the legal structure of Germany yet. Consequently, the scientists of the ILEWS project took over the role of the operating experts with editing rights.

Discussion

Inevitably, uncertainties remain in the application of CHASM which derive principally from the estimation of subsurface conditions, geotechnical characteristics and groundwater positions, and the influence of expert judgement in their estimation. The determination of the spatial extent of subsurface materials was based on a range of input data to create a high-quality representation of the subsurface conditions. In particular, seismic refraction was demonstrated to be a cost-effective and time-saving data acquisition approach. The utilisation of literature sources for the estimation of geotechnical properties provided parameter values that could be calibrated by extensive CHASM simulations and proved sufficient for the demonstration of our methodology. However, for an effective early warning system, the geomechanical characterisation should be carried out by the application of more reliable techniques such as shear tests of field samples. The assessment of groundwater positions relied on an extensive hydrological monitoring system. However, the estimation of groundwater scenarios proved to be difficult due to sometimes contradictory measurements and the complex subsurface hydrology which features preferential flow paths. Nevertheless, annual minimum and maximum groundwater elevations could be determined with relatively high reliability.

Overall, the results of CHASM modelling infer a relatively low stability for some parts of the study area. In particular, the shear surfaces located close to the damaged house resulted in low FoS values. These CHASM outputs are in agreement with the largest displacements measured by inclinometers. Nonetheless, for the upper slope areas there is no evidence of large displacements. According to the results of CHASM modelling, subsequent heavy rainfall, or snow melt events, could lead to a reduction of shear resistance to critical levels. However, precise thresholds of the conditions which would lead to a reactivation of slope movement are difficult to determine due to the complex subsurface conditions and preferential flow pathways. Of the two types of landslide movement inferred from the inclinometers, deep-seated sliding on the bedrock interface, and shallower flow-like and time-dependent displacement, only the former can be simulated using limit-equilibrium models

such as CHASM. In common with most landslide early warning systems implemented elsewhere, this implementation uses thresholds of monitored landslide characteristics (e.g. displacement rates) for issuing warnings. However, in addition, monitoring data is also fed into the CHASM WPS model to predict the future slope stability conditions, thus extending the potential warning time. The implemented CHASM early warning model prototype aimed to assess the feasibility of such an approach. With respect to this goal, the study was successful, even though no practical early warnings can currently be issued due to the lack of real-time rainfall forecasts. However, if stakeholders demanded realistic warnings, and precipitation data were provided, the technical system could easily be modified to integrate these.

Conclusions

This study presents the application of the limit-equilibrium model CHASM to a reactivated and extremely slow moving landslide in the Swabian Alb, as well as the subsequent implementation of the model into a semi-automated and expert-controlled early warning system.

The landslide analysed in this study is on a slope typical of the Swabian Alb region, which features many slow-moving landslides. Even though the landslide currently does not show signs of an imminent failure, the potential damage would be significant for the local community should failure occur. Moreover, in a more general context, the success of this demonstration suggests the methodology is applicable to areas in which the need for landslide early warning is more critical from the standpoint of all aspects of landslide risk (hazard, exposure and vulnerability).

Cooperative planning of the layout of the early warning system, including the visualisation of monitoring and modelling results, and the dissemination of warnings, with local and regional decision-makers, greatly facilitated the entire system which would otherwise have been differently configured, if only scientists had been involved in the design. This demand-orientated approach was important for securing acceptance of the early warning system, as well as in respect of the associated legal responsibilities. As a result, a three-colour traffic light code was implemented in which the highest level can only be reached following authorisation from an expert (and not automatically).

The utilisation of open-source software and international OGC standards is an important condition for the interoperability of the system and for other landslide early warning applications. Importantly, the implementation of CHASM as a WPS shows the potential of this service to integrate complex simulation algorithms into web-based geospatial applications. In addition, the notification service, based on the WNS standard, is an ideal solution for integrating several alert thresholds for monitoring sensors and modelling results, as well as providing automated notifications to experts using different communication channels.

The direct implementation of CHASM as an early warning model is a novel approach in which early warnings are not solely based on expert interpretation of monitoring data or pre-defined threshold values, but also on the direct integration of frequently used slope stability software. In the early warning system, CHASM fulfils two purposes: it serves as an automated model which forecasts slope stability and subsequently notifies experts on potentially dangerous

conditions, and it can be used to verify alerts issued due to the exceedance of pre-defined thresholds relating to monitoring sensors. The developed prototype methodology demonstrates the technical feasibility of using physically based predictions of slope stability as part of a landslide early warning system. It can be expected that future endeavours in the field of landslide early warning will utilise similar approaches, and thus the integration of slope stability analysis models within early warning systems will increase the reliability of any warnings that are issued. Additionally, the results from the prototype system designed and reported here suggest that future research should also develop web processing systems that encompass a range of constitutive model formulations for slope stability, together with the inclusion of uncertainty in the hydrogeological model

Acknowledgements

We would like to thank the German Ministry of Education and Research for funding the ILEWS project (No. 03Go653A-03Go653F). We are grateful to LUBW, LGRB and DWD for providing essential data and thank the administration of Lichtenstein-Unterhausen for their cooperation. Additional support was granted by the 51st Chinese PostDoc Science Foundation (No.2012M511298). We also like to thank two anonymous reviewers for their helpful comments.

References

Anderson M, Holcombe L, Flory R, Renaud J-P (2008) Implementing low-cost landslide risk reduction: a pilot study in unplanned housing areas of the Caribbean. *Nat Hazard* 47:297–315. doi:10.1007/s11069-008-9220-z

Anderson MG, Lloyd DM, Park A, Hartshorne J, Othman A (1996) Establishing new design dynamic modelling criteria for tropical cut slopes. In: Senneset K (ed) *Landslides, 7th International Symposium on Landslides*. Balkema, Rotterdam, pp 1067–1072

Anderson MG, Richards K (1987) Modelling slope stability: the complementary nature of geotechnical and geomorphological approaches. In: Anderson MG (ed) *Slope stability: geotechnical engineering and geomorphology*. Wiley, New York, pp. 1–9

Anderson SA, Thallapally LK (1996) Hydrologic response of a steep tropical slope to heavy rainfall. In: Senneset K (ed) *Landslides, 7th International Symposium on Landslides*. Balkema, Rotterdam, pp 1489–1495

Aslan AM, Burghaus S, Li L, Schauerer W, Kuhlmann H (2010) Bewegungen an der Oberfläche. In: Bell R, Mayer J, Pohl J, Greiving S, Glade T (eds) *Integrative Frühwarnsysteme für gravitative Massenbewegungen (ILEWS) Monitoring, Modellierung, Implementierung*. Klartext, Essen, pp 74–84

Badoux A, Graf C, Rhyner J, Kuntner R, McArdell BW (2009) A debris-flow alarm system for the Alpine Illgraben catchment: design and performance. *Nat Hazard* 49:517–539. doi:10.1007/s11069-008-9303-x

Barla G, Amici R, Vai L, Vanni A (2004) Investigation, monitoring and modelling of a landslide in porphyry in a public safety perspective. In: Lacerda W, Ehrlich M, Fontoura SAB, Sayao AS (eds) *Landslides: evaluation and stabilization, 9th International Symposium on Landslides*. Balkema, Leiden, pp 623–628

Bartels H, Dietzer B, Malitz G, Albrecht FM, Guttenberg J (2005) KOSTRA-DWD-2000. Starkniederschlagshöhen für Deutschland (1951–2000). Fortschreibungsbericht. Deutscher Wetterdienst (DWD), Abteilung Hydrometeorologie, Offenbach, Germany

Bear J (1972) *Dynamics of fluids in porous media*. Dover, New York

Bell R (2007) *Lokale und regionale Gefahren- und Risikoanalyse gravitativer Massenbewegungen an der Schwäbischen Alb*. Dissertation. University of Bonn, Germany

Bell R, Kruse J-E, Garcia A, Glade T, Hördt A (2006) Subsurface investigations of landslides using geophysical methods—geo-electrical applications in the Swabian Alb (Germany). *Geographica Helvetica* 201–208.

Bell R, Mayer J, Pohl J, Greiving S, Glade T (2010a) *Integrative Frühwarnsysteme für Gravitative Massenbewegungen (ILEWS)—Monitoring, Modellierung, Implementierung*. Klartext, Essen

Bell R, Wiebe H, Krummel H (2010b) Vorerkundung. In: Bell R, Mayer J, Pohl J, Greiving S, Glade T (eds) *Integrative Frühwarnsysteme für gravitative Massenbewegungen (ILEWS) Monitoring, Modellierung, Implementierung*. Klartext, Essen, pp 62–69

Beven KJ (1985) Distributed models. In: Anderson MG, Burt TB (eds) *Hydrological forecasting*. Wiley, New York, pp 405–435

Bibus E (1986) Die Rutschung am Hirschkopf bei Mössingen (Schwäbische Alb). *Geowissenschaftliche Rahmenbedingungen—Geökologische Folgen Geokodynamik* 333–360

Bibus E (1999) Vorzeitige, rezente und potentielle Massenbewegungen in SW-Deutschland—Synthese des Tübinger Beitrags zum MABIS-Projekt. In: Bibus E, Terhorst B (eds) *Angewandte Studien zu Massenbewegungen*. pp 1–57

Bishop AW (1955) The use of the slip circle in the stability analysis of slopes. *Geotechnique* 5:7–17

Bleich KE (1960) Das Alter des Albtraufs. *Jahreshefte des Vereins für Vaterländische Naturkunde in Württemberg* 115:39–92

Blikra LH (2008) The Aknes rockslide; monitoring, threshold values and early-warning. *Landslides and engineered slopes. From the past to the future. Proceedings of the 10th International Symposium on Landslides and Engineered Slopes*, pp. 1089–1094

Camek T, Becker R, Öhl S (2010) Bodenfeuchte (TDR, Tensiometer). In: Bell R, Mayer J, Pohl J, Greiving S, Glade T (eds) *Integrative Frühwarnsysteme für gravitative Massenbewegungen (ILEWS) Monitoring, Modellierung, Implementierung*. Klartext, Essen, pp 92–100

Cannata M, Luan TX, Molinari ME, Long NH (2010) WPS application for shallow landslide hazard assessment. *Geoinformatics for Spatial-Infrastructure Development in Earth and Allied Sciences (GIS-IDEAS) 2010*

Capparelli G, Tiranti D (2010) Application of the MoniFlaLR early warning system for rainfall-induced landslides in Piedmont region (Italy). *Landslides* 4:401–410

Chung C (2008) Predicting landslides for risk analysis—spatial models tested by a cross-validation technique. *Geomorphology* 94:438–452. doi:10.1016/j.geomorph.2006.12.036

Clark AR, Moore R, Palmer JS (1996) Slope monitoring and early warning systems: application to coastal landslide on the south and east coast of England, UK. In: Senneset K (ed) *Landslides, 7th International Symposium on Landslides*. Balkema, Rotterdam, pp 1531–1538

Collison AJC, Anderson MG (1996) Using a combined slope hydrology/stability model to identify suitable conditions for landslide prevention by vegetation in the humid tropics. *Earth Surf Process Landforms* 21:737–747

Consortium for Small Scale Modeling (2007) Operations at DWD—COSMO-DE. http://www.cosmo-model.org/content/tasks/operational/dwd/default_de.htm. Accessed 24 Jan 2011

Cruden DM, Varnes DJ (1996) Landslide types and processes. In: Turner AK, Schuster RL (eds) *Landslides: investigation and mitigation (special report)*, Transportation and Research Board Special Report 247. National Research Council, Washington D.C., pp 36–75

Deutscher Wetterdienst (2010b) COSMO. <http://goo.gl/f47Cz>. Accessed 24 Jan 2011

Deutscher Wetterdienst (2010a) *Wettervorhersagemodelle*. <http://goo.gl/Gu9v3>. Accessed 24 Jan 2011

Dikau R, Brunsden D, Schrott L, Ibsen ML (eds) (1996) *Landslide recognition: identification, movement and causes: identification, movement and causes*. Wiley, Chichester

Dikau R, Weichselgartner J (2005) *Der unruhige Planet. Der Mensch und die Naturgewalten*. Primus, Darmstadt

Ferentinou MD, Sakellariou M, Matziaris V, Charalambous S (2006) An introduced methodology for estimating landslide hazard for seismic and rainfall induced landslides in a geographical information system environment. In: Nadim F, Pöttler R, Einstein H, Klapperich H, Kramer S (eds) *Geohazards*. Lillehammer, Norway, pp 1–8

Forchheimer P (1930) *Hydraulik*. Teubner, Leipzig

Froese CR, Murray C, Cavers DS, Anderson WS, Bidwell AK, Read RS, Cruden DM, Langenberg W (2005) Development and implementation of a warning system for the South Peak of Turtle Mountain. In: Hungr O, Fell R, Couture R, Eberhardt E (eds) *International Conference on Landslide Risk Management*. Taylor & Francis, Vancouver, pp 705–712

Fundinger A (1985) *Ingenieurgeologische Untersuchung und geologische Kartierung (Dogger/Malm) der näheren Umgebung der Rutschungen am Hirschkopf bei Mössingen und am Irenberg bei Thanheim (Baden-Württemberg)*. Geowissenschaftliche Fakultät, University Tübingen, Tübingen

Goetz JN, Guthrie RH, Brenning A (2011) Integrating physical and empirical landslide susceptibility models using generalized additive models. *Geomorphology* 129(3–4):376–386

- Greiving S (2010) Risikomanagement. In: Bell R, Mayer J, Pohl J, Greiving S, Glade T (eds) Integrative Frühwarnsysteme für gravitative Massenbewegungen (ILEWS) Monitoring, Modellierung, Implementierung. Klartext, Essen, pp. 203–230
- Guzzetti F, Reichenbach P, Cardinali M, Galli M, Ardizzone F (2005) Probabilistic landslide hazard assessment at the basin scale. *Geomorphology* 72:272–299. doi: 10.1016/j.geomorph.2005.06.002
- Ho KKS, Lau JWC (2010) Learning from slope failures to enhance landslide risk management. *Q J Eng Geol Hydrogeol* 43:33–68
- Iovine GGR, Lollino P, Gariano SL, Terranova OG (2010) Coupling limit equilibrium analyses and real-time monitoring to refine a landslide surveillance system in Calabria (southern Italy). *Nat Hazards Earth Syst Sci* 10:2341–2354. doi:10.5194/nhess-10-2341-2010
- Jäger S, Paulsen H, Mayer C, Huber B, Dietz R, Greve K, Camek T (2010) Informationstechnik in der Frühwarnmodellierung. In: Bell R, Mayer J, Pohl J, Greiving S, Glade T (eds) Integrative Frühwarnsysteme für gravitative Massenbewegungen (ILEWS) Monitoring, Modellierung, Implementierung. Klartext, Essen, pp 155–179
- Jäger S, Thiebes B, Bell R, Glade T (2012) Applying geospatial web standards for real-time on-line slope stability modeling as a basis for a landslide early warning system. Proceedings of the 11th International & 2nd North American Symposium on Landslides
- Janbu N (1996) Slope stability evaluations in engineering practice. In: Senneset K (ed) Landslides, 7th International Symposium on Landslides. Balkema, Rotterdam, pp 17–34
- Janbu N (1954) Application of composite slip surface for stability analysis. Proceedings of the European Conference on the Stability of Earth Slopes. pp 43–49
- Kallinich J (1999) Verbreitung, Alter und Ursachen von Massenverlagerungen an der Schwäbischen Alb auf der Grundlage von geomorphologischen Kartierungen. In: Bibus E, Terhorst B (eds) Angewandte Studien zu Massenbewegungen. pp 59–82
- Konikow LF, Bredehoft JD (1992) Groundwater models cannot be validated. *Adv Water Resour* 15:75–83
- Krauter E (1992) Hangrutschungen – Ein Umweltproblem. Conference paper @ Ingenieurvermessung 1992. XI. Internationaler Kurs Für Ingenieurvermessung. Zürich, Switzerland. Eidgenössische Technische Hochschule (ETH) Zürich:1–12.
- Krauter E, Lauterbach M, Feuerbach J (2007) Hangdeformationen–Beobachtungsmethoden und Risikoanalyse. *Geo-international & Forschungsstelle Rutschungen* 1–6.
- Kreja R, Terhorst B (2005) GIS-gestützte Ermittlung rutschungsgefährdeter Gebiete am Schönberger Kapf bei Öschingen (Schwäbische Alb). *Die Erde* 136:395–412
- Kruse JE (2006) Untergrunderkundung und Monitoring von gravitativen Massenbewegungen mit Gleichstromgeoelektrik und Radiomagnetotellurik. Unpublished master thesis. University of Bonn, Germany
- Lateh H, Anderson MG, Ahmad F (2008) CHASM—the model to predict stability of gully walls along the east–west highway in Malaysia: a case study. Proceedings of the First World Landslide Forum. ISDR, Tokyo, Japan, pp. 340–343
- Lauterbach M, Krauter E, Feuerbach J (2002) Satellitengestütztes Monitoring einer Großrutschung im Bereich eines Autobahndammes bei Landstuhl/Pfalz. *Geotechnik* 25:97–100
- Leser H (1982) Erläuterungen zur Geomorphologischen Karte 1:25,000 der Bundesrepublik Deutschland. GMK 25 Blatt 9 7520 Mössingen Geomorphologische Detailkartierung in der Bundesrepublik Deutschland. Geo Center, Stuttgart, Germany
- Macfarlane DF, Sylvester PK, Benck JM, Whiford ND (1996) Monitoring strategy and performance of instrumentation in the clyde power project landslide, New Zealand. In: Senneset K (ed) Landslides (Glissements de Terrain): Proceedings of the 7th International Symposium, Trondheim, Norway, 17–21 June 1996. Taylor & Francis, London, pp. 1557–1564
- Malitz G (2005) KOSTRA-DWD-2000. Starkniederschlagshöhen für Deutschland (1951–2000). Grundlagenbericht. Deutscher Wetterdienst (DWD), Hydrometeorologie, Offenbach, Germany
- Matziaris VG, Ferentinou M, Sakellariou MG (2005) Slope stability in unsaturated soils under static and rainfall conditions. *Ovidius Univ Ann Ser Civ Eng* 1:103–110
- Mayer J, Pohl W (2010) Risikokommunikation. In: Bell R, Mayer J, Pohl J, Greiving S, Glade T (eds) Integrative Frühwarnsysteme für gravitative Massenbewegungen (ILEWS) Monitoring, Modellierung, Implementierung. Klartext, Essen, pp 180–202
- Meyenfeld H (2009) Modellierungen seismisch ausgelöster gravitativer Massenbewegungen für die Schwäbische Alb und den Raum Bonn und Erstellen von Gefahrenhinweiskarten. Dissertation. University of Bonn, Germany
- Millington RJ, Quirk JP (1959) Permeability of porous media. *Nature* 183:387–388
- Muir-Wood D (2004) Geotechnical modelling. Taylor and Francis, London
- Muir-Wood D, Mackenzie NL, Chan AHC (1993) Selection of parameters for numerical predictions. In: Predictive soil mechanics. Proceedings of the Wroth Memorial symposium, St Catherine's College, Oxford. Thomas Telford, pp. 496–512
- Neuhäuser B, Terhorst B (2007) Landslide susceptibility assessment using “weights-of-evidence” applied to a study area at the Jurassic escarpment (SW-Germany). *Geomorphology* 86:12–24
- Ohmert W, Von Koenigswald W, Münzing K, Villinger E (1988) Geologische Karte 1:25.000 von Baden Württemberg. Erläuterungen zu Blatt 7521 Reutlingen
- Palm H, Staab S, Schmitz R (2003) Verkehrssicherheiten an klassifizierten Straßen im Hinblick auf Steinschlag- und Felssturzgefahr. Rutschungen in Rheinland-Pfalz. Erkennen, Erkunden und Sanieren. Felsicherung und Sanierung von Stützmauern. Mainz, Germany, pp. 16–22
- Papathoma-Köhle M, Neuhäuser B, Ratzinger K, Wenzel H, Dominey-Howes D (2007) Elements at risk as a framework for assessing the vulnerability of communities to landslides. *Nat Hazards Earth Syst Sci* 7:765–779
- Richards LA (1931) Capillary conduction of liquids through porous mediums. *Physics* 1:318–333
- Rossi M, Guzzetti F, Reichenbach P, Mondini AC, Peruccacci S (2010) Optimal landslide susceptibility zonation based on multiple forecasts. *Geomorphology* 114:129–142
- Ruch C (2009) Georisiken. Aktive Massenbewegungen am Albrauf. LGRB-Nachrichten 8:1–2
- Sakellariou M, Ferentinou M, Charalambous S (2006) An integrated tool for seismic induced landslide hazards mapping. In: Agioutantis Z, Komnitsas K (eds) First European Conference on Earthquake Engineering and Seismology. Geneva, Switzerland, pp. 1365–1375
- Sass O, Bell R, Glade T (2008) Comparison of GPR, 2D-resistivity and traditional techniques for the subsurface exploration of the Öschingen landslide, Swabian Alb (Germany). *Geomorphology* 93:89–103
- Saxton KE, Rawls WJ (2006) Soil water characteristic estimates by texture and organic matter for hydrologic solutions. *Soil Sci Soc Am J* 5:1569–1578
- Saxton KE, Willey MP (2006) The SPAW model for agricultural field and pond hydrologic simulation. In: Singh VP, Frevert D (eds) Mathematical modeling of watershed hydrology. CRC, Boca Raton, pp. 401–435
- Schädel K, Stober I (1988) Rezente Großrutschungen an der Schwäbischen Alb. Jahreshefte des Geologischen Landesamtes Baden-Württemberg 431–439
- Schut P (2007) OpenGIS Web Processing Service: OGC 05-007r7: Version 1.0. 0. Open Geospatial Consortium Inc.
- Simonis I, Echterhoff J (2006) Draft OpenGIS® Web Notification Service Implementation Specification.
- Sirangelo B, Braca G (2004) Identification of hazard conditions for mudflow occurrence by hydrological model: application of FLalR model to Sarno warning system. *Eng Geol* 73:267–276
- Stähli M, Bartel P (2007) Von der Auslösung zur Massenbewegung. In: Hegg C, Rhyner J (eds) Warnung bei aussergewöhnlichen Naturereignissen. pp 33–38
- Sung CT, Iba J (2010) Accuracy of the Saxton–Rawls method for estimating the soil water characteristics for mineral soils of Malaysia. *Pertanika J Trop Agric Sci* 33:297–302
- Terhorst B (1997) Formenschatz, Alter und Ursachenkomplexe von Massenverlagerungen an der schwäbischen Juraschichtstufe unter besonderer Berücksichtigung von Boden- und Deckschichtenentwicklung, Tübingen
- Terhorst B, Kreja R (2009) Slope stability modelling with SINMAP in a settlement area of the Swabian Alb. *Landslides* 6:309–319. doi:10.1007/s10346-009-0167-2
- Thiebes B (2011) Landslide analysis and early warning—local and regional case study in the Swabian Alb, Germany. Dissertation. University of Vienna, Austria
- Thiebes B (2012) Landslide analysis and early warning systems: local and regional case study in the Swabian Alb. Springer, Berlin
- Turner AK (1996) Socioeconomic significance of landslides. In: Turner AK, Schuster RL (eds) Landslides: investigation and mitigation (special report). Transportation Research Board, pp. 12–35
- UMS (2007) Bedienungsanleitung T8 Langzeitmonitoring-Tensiometer. UMS, München
- Wiebe H, Krummel H (2010) Bodenfeuchte (Geoelektrik). In: Bell R, Mayer J, Pohl J, Greiving S, Glade T (eds) Integrative Frühwarnsysteme für gravitative Massenbewegungen (ILEWS) Monitoring, Modellierung, Implementierung. Klartext, Essen, pp 100–116

- Wiebe H, Krummel H, Camek T, Thiebes B (2010) Kombinierte Auswertung der Bodenfeuchte. In: Bell R, Mayer J, Pohl J, Greiving S, Glade T (eds) *Integrative Frühwarnsysteme für gravitative Massenbewegungen (ILEWS) Monitoring, Modellierung, Implementierung*. Klartext, Essen, pp 116–129
- Wilkinson PL, Anderson MG, Lloyd DM (2002a) An integrated hydrological model for rain-induced landslide prediction. *Earth Surf Process Landforms* 27:1285–1297. doi:10.1002/esp.409
- Wilkinson PL, Anderson MG, Lloyd DM, Renaud JP (2002b) Landslide hazard and bioengineering: towards providing improved decision support through integrated numerical model development. *Environ Model Softw* 17:333–344
- Wilkinson PL, Brooks SM, Anderson MG (2000) Design and application of an automated non-circular slip surface search within a combined hydrology and stability model (CHASM). *Hydrol Processes* 14:2003–2017
- Willenberg H, Spillmann T, Eberhardt E, Evans KF, Loew H, Maurer H (2002) Multidisciplinary monitoring of progressive failure process in brittle rock slopes—concepts and system design. In: Jan Rybář J, Stemberk J, Wagner P (eds) *Landslides: proceeding of the First European Conference on Landslides*. Balkema, Prague, pp 477–483
- Yin Y (2009) Landslide mitigation strategy and implementation in China. In: Sassa K, Canuti P (eds) *Landslides—disaster risk reduction*. Springer, Berlin, pp 482–484
- Yin Y, Wang H, Gao Y, Li X (2010) Real-time monitoring and early warning of landslides at relocated Wushan Town, the Three Gorges Reservoir, China. *Landslides* 7:339–349. doi:10.1007/s10346-010-0220-1

B. Thiebes (✉)

School of Geography Science,
Nanjing Normal University,
No. 1 Wenyuan Road, Nanjing 210046, People's Republic of China
e-mail: Benni.Thiebes@gmail.com

R. Bell · T. Glade

Department of Geography and Regional Research,
University of Vienna,
Universitaetsstr. 7, 1010 Vienna, Austria

S. Jäger

Geomer GmbH,
Im Breitspiel 11 b, 69126 Heidelberg, Germany

J. Mayer

Department of Geography,
University of Bonn,
Meckenheimer Allee 166, 53115 Bonn, Germany

M. Anderson · L. Holcombe

Department of Civil Engineering,
University of Bristol,
Queen's Building, University Walk, Bristol BS8 1TR, UK